

## Unsteadiness and Spatio-Temporal Statistics in Intermediate Effervescent Spray Region

Miloslav Dohnal\*, Jiří Hájek, Jiří Vondál

Brno University of Technology, Faculty of Mechanical Engineering, Institute of Process and Environmental Engineering, Technická 2, 616 69 Brno, Czech Republic  
 dohnal@upei.fme.vutbr.cz

Multipoint statistics theory of the ideal spray was used to investigate temporal spray stability. The analysis focused on intermediate spray region, i.e. between dense and self-similar regions. Arrival time and diameter are the studied characteristics of the droplets. Two size classes, with droplet diameters of 50 and 100  $\mu\text{m}$ , were selected for steadiness analysis. The two size classes were used to investigate temporal droplet behaviour using their arrival time. Chi-square test was used to provide unsteadiness criterion. Data were collected by dual-phase Doppler anemometry (PDA) at three planes perpendicular to the spray axis ( $x/D = 20, 40, 60$ ). At each plane, there were several measuring points spanning the spray radius, starting from the spray centreline ( $r/x = 0$ ) to the spray cone boundary ( $r/x = 0.5$ ). The effervescent breakup mechanism is shown to produce spray unsteadiness, which is however significant only away from spray axis. In a narrow cone around the spray axis, the spray is steady on a significance level of 5 %. This result provides guidance for assessment of effervescent spray unsteadiness. The data show unexpectedly similar levels of unsteadiness for gas-liquid ratios between 5 and 15 %. This has implications for combustion applications of effervescent spray, where unsteadiness is an undesirable property.

### 1. Introduction

In the field of combustion, effervescent breakup mechanism was first introduced by Lefebvre et al. (1988) and it gradually become very popular. It is realized by twin-fluid atomiser with internal mixing, the fluid to be atomised is mixed with atomizing gas inside the nozzle and two phase flow occurs. As liquid-gas mixture leaves the nozzle via the exit orifice, the drop in pressure causes gas expansion that atomises the liquid into discrete fragments (filaments and droplets) in the primary atomization region (Lefebvre et al., 1988). The breakup mechanism works well with relatively low injection pressures and large diameters of the exit orifice, without compromising the size of drops (Babinsky and Sojka, 2002) and while increasing the spray angle as compared to plain-orifice pressure atomisers (Chen and Lefebvre, 1994).

Gas flow rate is very small in comparison with liquid flow rate, mostly below 20 % gas-liquid ratio (GLR). The injection pressure and GLR influence the two-phase flow regime of the mixture inside the nozzle. Jedelský and Jícha (2008) published modified Baker's map, where transition between flow regimes can be predicted – bubbly, slug and annular flow. The non-uniformity of gas and liquid phase inside the nozzle and due to bubble rapid expansion leads to different fragment diameters (Sovani et al., 2001). Outside of the discharge orifice (dense region), the liquid is ripped apart in every direction by expanding bubbles. In the far-field (dilute region), the spray is fully developed (no ligaments can be seen). The droplets are slowed down by aerodynamic drag force and can collide or coalesce.

During literature review, several mutually inconsistent definitions of various spray regions have been found. This paper adopts and refines definitions introduced by Linne (2013). The dense region thus lies directly downstream from the discharge orifice and is characterised by the presence of liquid ligaments. When all ligaments disintegrate by primary atomization into droplets, Linne (2013) calls the spray dilute. Previous work on spatial and temporal behaviour of droplets investigated spray in a region where spray is self-similar ( $x/D > 100$ ), see (Panchagnula and Sojka, 1999). There is a lack of information of droplet behaviour in the intermediate region lying between the dense and the self-similar region. This is therefore

the focal area investigated in this paper. Spatial spray behaviour analysis of unsteadiness in the intermediate region is done by adopting multipoint statistical method introduced in (Edwards and Marx, 1995a) as conceptual method and in (Edwards and Marx, 1995b) as an application.

## 2. Experimental Apparatus and Setup

The experimental data explored in this paper were previously discussed from a perspectives by Broukal and Hájek, (2014). This paper provides deeper experimental data analysis; and further extends spray unsteadiness research partially described in Hájek et al. (2015).

The experiments were done using a vertically positioned effervescent atomiser described in detail as design E38 by (Jedelský et al., 2009). For the measurements, dual Phase Doppler Anemometry (PDA) approach was used, from Dantec Dynamics A/S. Spray measurements analysed in this work were done with varying gas-liquid ratio. Each experimental condition was measured at three perpendicular planes to atomiser axis with different dimensionless distance from the exit orifice ( $x/D = 20, 40, 60$ ). The nozzle diameter was  $D = 2.5 \text{ mm}$  and plane distances from the exit orifice were 50, 100 and 150 mm. At each plane, measurements were carried out with varying dimensionless radial distance from the spray axis  $r/x$ , starting from the spray centreline ( $r/x = 0$ ) to the edge of the spray ( $r/x = 0.5$ ). This approach resulted in 17 measurement points, where data were collected for each spray.

### 2.1 Operating Conditions

This paper puts emphasis on a set of operating conditions with fixed liquid flow rate of 31.2 kg/h, with three levels of GLR. The operating conditions used for the investigation are shown in Table 1 below.

Table 1: Operating conditions

#	Liquid Pressure [Pa(g)]	Air Pressure [Pa(g)]	Liquid Flow Rate [kg/h]	Gas Flow Rate [kg/h]	GLR [-]
1	34,473.79	55,158.06	31.20	1.56	0.05
2	89,631.84	144,100.40	31.20	3.12	0.10
3	144,789.90	234,421.40	31.20	4.68	0.15

## 3. Theory

As mentioned above, the Edward's and Marx's (1995a and 1995b) multipoint statistic method was chosen for the investigation of temporal behaviour droplets. The adopted theory of spray unsteadiness is based mainly on time sequence behaviour. For this purpose, the droplet arrival time into the measurement volume is used. In terms of the independent variable (time) the ideal (sometimes called steady) spray is considered to obey inhomogeneous Poisson statistics. Unsteady sprays are those, whose interparticle distribution function does not obey inhomogeneous Poisson statistics (Luong and Sojka, 1999).

The idea is to break down measuring time interval into a number of sub-sequences according to Eq(2). The droplets are monitored with their arrival time. This is well-described by Poisson distribution that expresses the probability that certain number of events will occur during fixed interval of time (measuring time) and/or space (measuring points).

### 3.1 Interparticle Distribution Function

Edwards and Marx (1995a and 1995b) introduced formalism to evaluate if the investigated spray is steady or not. The formalism can be summarised as follows. First, measure the interparticle arrival times for the spray and create its histogram. Then assume the spray is steady and calculate the probability density function and construct corresponding function; finally, compare the two.

First of all, interparticle time probability density is determined from the experiment. The possible ways how to measure interparticle arrival time are two – single long realisation (SR) or averaging of ensemble realisations (ER). Edwards and Marx developed the theory and proved that the experimental distribution density is the same for both types of realisations, assuming the spray operating conditions are constant. The experimental distribution function is described as follows (Edwards and Marx, 1995b):

$$h_{exp}(\tau_j) = \frac{H(\tau_j)}{N\Delta\tau_j} \quad (1)$$

where  $\tau_j$  [s] is interparticle time gap;  $N$  [-] is the number of interparticle events in a class;  $\Delta\tau_j$  [s] is the width of the  $j$ -th interparticle time gap and it is determined as time between two droplets;  $H(\tau_j)$  [-] is found by monitoring the number of droplets that fall within the interval  $\tau_j$ .

The binning of interparticle time was done according to Sojka's derivation of interparticle distribution function introduced by Edwards and Marx (Luong and Sojka, 1999):

$$\tau_j = T \left\{ 1 - \left[ \left( 1 - \frac{\tau_{j-1}}{T} \right)^{N/\theta} - \frac{1}{k} \right]^{\theta/N} \right\} \quad (2)$$

where  $N$  [-] is the number of interparticle events;  $\theta$  [-] is number of realisations;  $T$  [s] is total measuring time and  $k$  [-] represents number of bins ( $k$  was equal to 20 in this work).

Now it remains to define the theoretical (steady) spray probability density function to be used for comparison. As mentioned above, the spray behaviour is assumed to obey the Poisson distribution which is characterised by an intensity function  $\lambda$  (it is constant in our case). Intensity function symbolizes number of expected observations of droplets per time unit. Marx and Edwards (1995b) developed analytical formula for the ideal spray as follows:

$$h_{th} = \frac{(T - \tau)\lambda^2 e^{(-\lambda\tau)}}{\lambda T - 1 + e^{(-\lambda T)}} \quad (3)$$

Since the expression of single long and ensemble average realisations probability density function is the same, they have different proportion of validity. Edwards and Marx (1995a) defined the dimensionless sampling time for single long realisation, which is equal to accumulation density of droplets; for steady sprays  $\theta \equiv \Lambda(T) = \lambda T$ . As this sampling time becomes long ( $\theta \gg 1$ ), it can be expected that sufficient number of droplets are collected; leading to a representative and stable interparticle time histogram.

### 3.2 Steadiness judgment

Above, the method to determine interparticle time probability density function of the spray was introduced. Now, it is necessary to compare experimental and theoretical probability density functions to assess if the spray is steady or not at certain statistical significance. This is done by statistical hypothesis testing. Before decision can be done, proper hypothesis has to be defined. The null hypothesis is that the spray is steady, and alternative hypothesis is that it is not steady. In statistics, there are several methods to evaluate match between those two probability density functions. Edward and Marx (1995b) refer especially to Kolmogorov-Smirnov and chi-square tests. For further information of Kolmogorov-Smirnov test, see Knuth (1981). This work is based on chi-square test used by Luong and Sojka (1999). In their work, they described and adjusted the chi-square analysis to evaluate match between probability density functions in the field of spray unsteadiness.

The chi-square test can be described as "the goodness of fit" test at certain significance level. In this work, the significance level  $\alpha$  of 5 % was chosen; and defines the acceptance region where the null hypothesis is considered true. The spray unsteadiness judgment is done by comparing calculated chi-square value and its critical value. If the determined chi-square value is less than the critical chi-square value, then the fit (steady curve) of the experimental distribution is good; resulting in null hypothesis acceptance. Chi-square values are determined using Luong's and Sojka's (1999) derivation of chi-square general formalism. Adjusted formula can be written as follows:

$$\chi^2 = \sum_{j=1}^k \frac{[H_j - N(e^{-\lambda L_j} - e^{-\lambda H_j})]^2}{N(e^{-\lambda L_j} - e^{-\lambda H_j})} \quad (4)$$

where  $L_j$  [s] is lower edge of the  $j$ -th bin and  $H_j$  [s] is the upper edge of the  $j$ -th bin.

First step in the classification is to divide the spray into sufficiently narrow size classes. Each droplet class is expected to exhibit a specific behaviour. The splitting could be done according to any marker that defines the droplet, e.g. velocity or diameter. In this work, the classes were formed by the droplet diameter. A different behaviour of small and large droplets is expected. Droplets with low Stokes number ( $St \ll 1$ ) follow air streamlines, whereas for droplets with high Stokes number ( $St \gg 1$ ) their inertia dominates and their trajectories are little affected by the flow. Size classes with short interval in droplet diameter are desirable to avoid masking of smaller droplets by bigger ones. Two diameter classes have been defined to analyse in this work namely,  $d = 50 \mu m \pm 1 \mu m$  and  $d = 100 \mu m \pm 1 \mu m$ .

4. Results and Discussions

Internal flow structures inside the atomiser tend to influence the droplets formation process and its behaviour. Varying GLR modifies the atomiser injection pressure. The changes in injection pressure influence bubble velocity and size inside the atomiser (Sen et al., 2014). Bubbly flow inside the atomiser is reached by  $GLR = 0.05$  (spray #1). With increasing GLR, The character of the two-phase flow changes and other flow regimes are assumed to occur for  $GLR = 0.1$  (spray #2) and  $GLR = 0.15$  (spray #3).

Figure 1 shows visualisation of the spray unsteadiness for two narrow ( $\pm 1 \mu m$ ) size classes (central diameter  $d = 50 \mu m$  on the left; central diameter  $d = 100 \mu m$  on the right), at an off-axis position. It is noticeable the behaviour of droplets in this particular location is not steady. This result is qualitatively similar for the other GLRs and other locations, which confirms inherent unsteadiness of the spray. The experimental and the theoretical curve differ substantially in shape mainly in the shortest interparticle time bins. For example, the small size class, spray #1;  $x/D = 60$ ;  $r/x = 0.3$  (Figure 1a), the smallest bin has population almost 4 times higher than is expected.

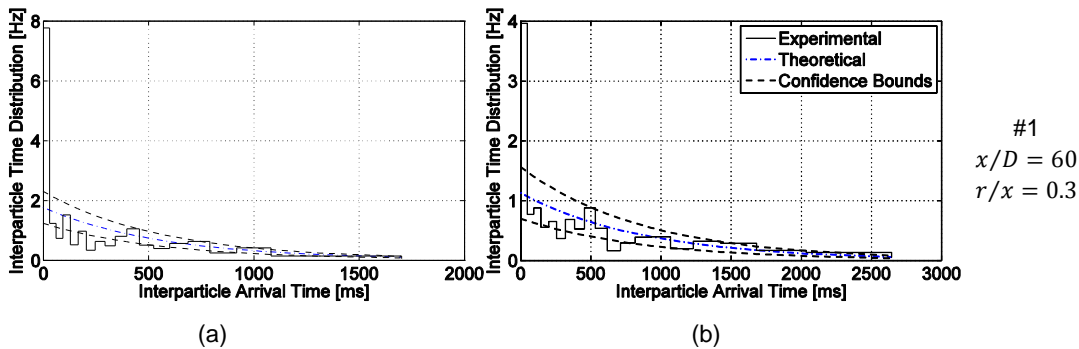


Figure 1: Comparison of the interparticle arrival time histogram and ideal (steady) distribution at  $GLR = 0.05$ ; (a) –  $50 \mu m \pm 1 \mu m$ ; (b) -  $100 \mu m \pm 1 \mu m$

Edward and Marx (1995b) noted several criticisms against spray unsteadiness presentation mentioned above. One of them, there is a lack of hard criterions for making judgment (only steady or unsteady criterions are available). They tried to compensate this deficiency by using expected deviation in bin height. This paper goes further and uses Luong’s and Sojka’s (1999) chi-square analysis to provide a clear boundary between steady and unsteady behaviour of droplets. The boundary between those two states is characterised by critical chi-square value. For this study (18 degrees of freedom; significance level  $\alpha$  equals to 5 %), the critical chi-square value is  $\chi_c^2 = 28.87$ .

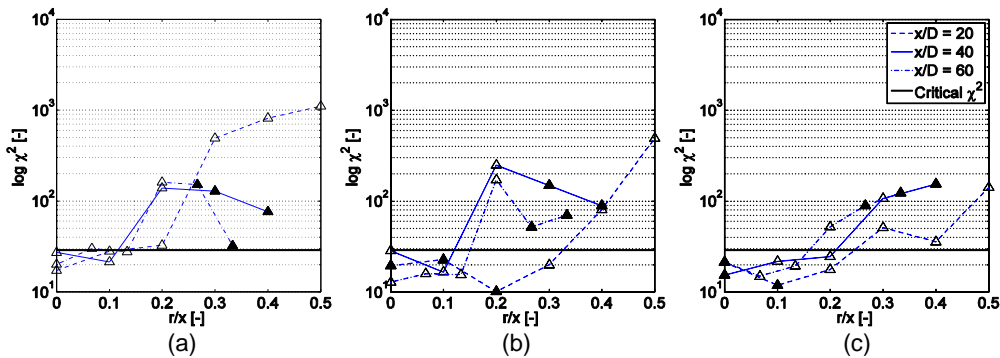


Figure 2: Visualisation of radial and axial chi-square evolution for size class  $d = 50 \mu m \pm 1 \mu m$ . (a) – spray #1; (b) – spray #2; (c) – spray #3

Figures 2 and 3 depict axial and radial evolution of chi-square values. Points under critical chi-square value (straight black line) represent steady behaviour of droplets. Black points, highlighted in Figure 2, and in the following figures, are less reliable due to low data quantity. At each measuring point, twenty interparticle arrival time bins have been constructed. At least 5 droplets have to be collected in each bin according to the chi-square test requirements. The highlighted points are those where at least one bin did not have cumulative count above 5 droplets. In Figure 2a, unreliability occurs in 23.53 %; in Figure 2b and 2c, there are 41.18 % points unreliable. It may be seen from the figures that the unreliable points clearly

lead to different trends of chi-square evolution across the spray radius than in cases where sufficient number of droplets was available.

It is further clear from the graphs that droplet unsteadiness tends to increase with radial/axial distance from the centreline and from the discharge orifice. Near the spray axis, the spray passes the steadiness criterion. This could be caused by entrainment of the droplets from the outer spray region. The entrainment is generated by high centreline velocity, see Hájek et al. (2015). On the spray edge, escalating unsteadiness in droplets behaviour can be seen. In case of droplets in the larger size class  $d = 100 \mu\text{m} \pm 1 \mu\text{m}$ , there are a lot of unreliable points. For the spray #1 (Figure 3a), unreliability occurs in 41.18 %; in Figure 3b, there are 35.29 % points under reliability; and for the spray #3 (Figure 3c), large number of points are not reliable – 58.82 %.

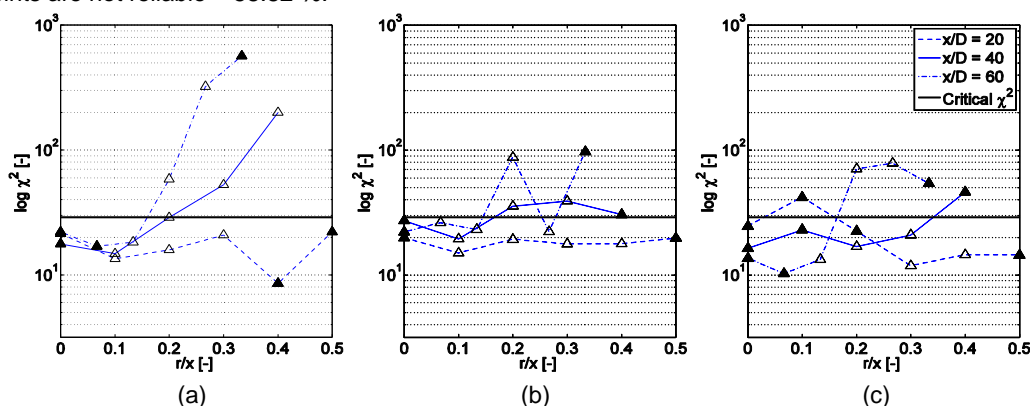


Figure 3: Visualisation of radial and axial chi-square evolution for size class  $d = 100 \mu\text{m} \pm 1 \mu\text{m}$ . (a) – spray #1; (b) – spray #2; (c) – spray #3

To avoid errors in judgment of spray steadiness due to insufficient number of droplets in individual bins, two options are possible. Firstly, the size classes can be extended. Secondly, additional measurements could enlarge statistic ensemble, which was however not viable in this work. Below results are presented for size classes with the same central diameters (50 and  $100 \mu\text{m}$ ) but wider ( $\pm 5 \mu\text{m}$ ). Due to space limitations, only the size class  $d = 100 \mu\text{m} \pm 5 \mu\text{m}$  is shown.

The unsteadiness of newly formed size class is shown in Figure 4. The spray unsteadiness differs from the narrow drop class and the number of unreliable points is much lower (only in Figure 3c, unreliability can be seen in 23.53 % of points). Comparing with Figure 3, it is seen that droplet behaviour near the spray axis remains steady. The droplets however start to behave unsteadily closer to the spray axis. Near the discharge orifice, the spray again appears to have a wider steady core. However, the spray loses steadiness towards the spray edge. In case of the narrow class, the spray was steady for most radial positions at plane  $x/D = 20$ . Varying GLR, the spray remains steady near the spray axis but chi-square values increase. Furthermore, the spray unsteadiness increases with increasing distance from nozzle orifice.

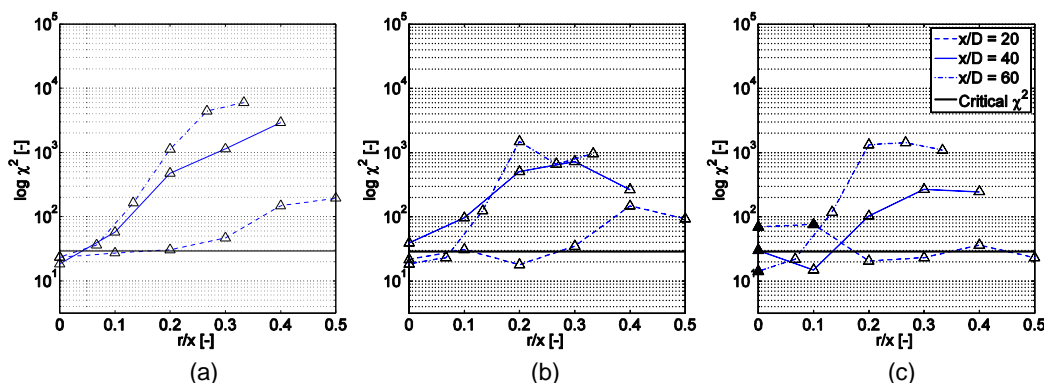


Figure 4: Visualisation of radial and axial chi-square evolution for size class  $d = 100 \mu\text{m} \pm 5 \mu\text{m}$ . (a) – spray #1; (b) – spray #2; (c) – spray #3

## 5. Conclusion

This work reports experimental results from an investigation of effervescent atomiser. The measurements were done by DANTEC dual-PDA analyser. The measurements provided two velocity components, droplet diameters and their arrival times. The present results use the raw data to describe the spatial evolution of spray unsteadiness. The spray was studied using the method developed by Luong and Sojka (1999) and Edwards and Marx (1995b). The spray was analysed in an intermediate spray region lying downstream from the dense spray area. Water and air served as the atomised liquid and atomizing gas. To obtain reliable results, the size classes had to be broadened to engulf sufficient number of collected droplets. An alternative that was prohibited by time and cost requirements would require radical extension of the measurements. Results of the work can be summarised as follows:

- The effervescent spray shows overall unsteady behaviour even at low GLR values
- Spray unsteadiness has a tendency to increase with growing axial and towards spray edge
- The spray satisfies steadiness criterion only in the measuring location nearest to the orifice
- We hypothesise that the improved steadiness near the spray axis is a result of entraining droplets from the outer spray region

## Acknowledgements

The research leading to these results has received funding from the Ministry of Education, Youth and Sports under the National Sustainability Programme I (Project LO1202). This work was also supported by the project CZ.1.07/2.3.00/30.0039 of Brno University of Technology.

## References

- Babinsky E., Sojka P.E., 2002, Modelling drop size distribution, *Progress in Energy and Combustion Science*, 28(4), 303-329.
- Broukal J., Hájek J., 2014, Experimental analysis of spatial evolution of mean droplet diameters in effervescent sprays, *Chemical Engineering Transactions*, 39, 781-786.
- Chen S.K., Lefebvre A.H., 1994, Spray cone angles of effervescent atomizers. *Atomization and Sprays*, 4, 291-301.
- Edwards C.F., Marx K.D., 1995a, Multipoint statistical analysis of the ideal spray, Part I: Fundamental concepts and the realization density, *Atomization and Sprays*, 5, 435-355.
- Edwards C.F., Marx K.D. 1995b, Multipoint statistical analysis of the ideal spray, Part II: Evaluating steadiness using the interparticle time distribution, *Atomization and Sprays*, 5, 457-505.
- Hájek J., Dohnal M., Vondál J., Broukal J., 2015, Analysis of effervescent spray quality for oil-fired furnace application, *Clean Technologies and Environmental Policy*, DOI: 10.1007/s10098-015-0922-0.
- Jedelský J., Jícha M., 2008, Unsteadiness in effervescent sprays: a new evaluation method and the influence of operational conditions, *Atomization and Sprays*, 18, 49-83.
- Lefebvre A.H., Wang X.F., Martin C.A., 1988, Spray characteristics of aerated-Liquid pressure atomizers, *Journal of Propulsion and Power*, 4(4), 293–298.
- Linne M., 2013, Imaging in the optically dense regions of a spray: a review of developing techniques, *Progress in Energy and Combustion Science*, 39, 403-440.
- Luong J.T.K, Sojka P.E., 1999, Unsteadiness in effervescent sprays, *Atomization and Sprays*, 9, 87-109.
- Panchagnula M.V., Sojka P.E., 1999, Spatial droplet velocity and size profiles in effervescent atomizer-produced sprays, *Fuel*, 78, 729-741.
- Sen D., Balzan M.,A., Nobes D.,S., Fleck B.,A., 2014, Bubble formation and flow instability in an effervescent atomizer, *Journal of Visualisation*, 2, 113-122.
- Sovani S.D., Sojka P.E., Lefebvre A.H., 2001, Effervescent atomization, *Progress in Energy and Combustion Science*, 27, 483-521.